University of Huddersfield

University of Huddersfield Repository

Cregan, Vincent and Lee, William

Slow and fast diffusion in a lead sulphate gravity separation process

Original Citation

This version is available at http://eprints.hud.ac.uk/id/eprint/34116/

http://eprints.hud.ac.uk/

PAPER • OPEN ACCESS

Slow and fast diffusion in a lead sulphate gravity separation process

To cite this article: Vincent Cregan and William T. Lee 2017 *J. Phys.: Conf. Ser.* **811** 012001

View the article online for updates and enhancements.

Slow and fast diffusion in a lead sulphate gravity separation process

Vincent Cregan[1,a], William T. Lee[2,b]

[1]Centre de Recerca Matemàtica, Campus de Bellaterra, Edifici C, 08193 Bellaterra, Barcelona, Spain

[2] Deptartment of Mathematics, University of Portsmouth, Winston Churchill Ave, Portsmouth PO1 2UP, UK

E-mail: [a]vcregan@crm.cat, [b]william.lee@port.ac.uk

Abstract. A model for the growth of lead sulphate particles in a gravity separation system from the crystal glassware industry is presented. The lead sulphate particles are an undesirable byproduct, and thus the model is used to ascertain the optimal system temperature configuration such that particle extraction is maximised. The model describes the evolution of a single, spherical particle due to the mass flux of lead particles from a surrounding acid solution. We divide the concentration field into two separate regions. Specifically, a relatively small boundary layer region around the particle is characterised by fast diffusion, and is thus considered quasi-static. In contrast, diffusion in the far-field is slower, and hence assumed to be time-dependent. The final system consisting of two nonlinear, coupled ordinary differential equations for the particle radius and lead concentration, is integrated numerically.

1. Introduction

Particle settling (or gravity separation) is a technique used in industry to separate liquid suspensions into one or more of its constitutive solid components by the action of gravity. Typical gravity separation industrial and medical applications include the removal of silt from industrial waste [1], the extraction of coal from material matter [2], gold refinery [3] and the division of blood into its fundamental components [4].

In the present study we consider a gravity settling method used to extract lead sulphate particles in acid polishing of lead crystal glassware. This process is currently used by an Irish glassware manufacturer and was originally presented at the 62nd European Study Group with Industry (ESGI62) [5]. The process begins with grinding where design cuts are inscribed onto the blank surfaces of the glass leaving it damaged and optically opaque. The damaged glass is then immersed in a polishing tank containing an aqueous solution of 65% sulphuric acid and 3% hydrofluoric acid. Chemical reactions between the acids and glass result in the formation of an insoluble lead sulphate layer at the glass surface. This layer obstructs the solution from reaching the glass, and hence the polishing performance deteriorates over time. Growth of the layer is counteracted by rinsing the glass regularly in an acidic-water solution. After rinsing, the solution is pumped into a large cone-shaped settlement tank where the lead sulphate particles settle out. The acid solution is cooled in the settlement tank such that the lead sulphate concentration decreases below the corresponding solubility limit in the polishing tank. This decrease in solubility results in both the precipitation of new small lead sulphate particles and

the growth of existing particles. However, the formation of the new particles is not desirable as they take longer to settle compared to existing particles. In addition, if the crystals are not given enough time to settle they are reintroduced back into the warmer polishing tank where they dissolve and bring the acid solution closer to saturation. After a period of time the acid solution once again becomes saturated and the insoluble lead sulphate layer reforms on the glassware. Repeated use of the settlement tank decreases the time for which the glassware can be polished effectively.

Previous particle settling studies have generally focussed on the dimensions of the settlement tank [1, 6], the fluid flow regime [7] or the introduction of an appropriate chemical agent [8]. The aim of this work is to investigate the often neglected influence that temperature has on gravity separation. In particular, we consider the effect of different temperature configurations on the growth of insoluble lead sulphate particles. We formulate a model for the evolution of a single, spherical lead sulphate particle due to the mass flux of lead atoms from the surrounding acid solution. We simplify the model to a system of two nonlinear ordinary differential equations for the lead concentration in the acid solution and the particle radius. We use this system to investigate the effect that three different temperature configurations have on process performance. Initially, we consider the current constant temperature regime where the initial temperature of the acid solution adjusts to the tank temperature. Following this we study the effect of cooling the acid solution at slower rates. Numerical solutions for the lead concentration and particle radius for each of the temperature regimes are presented. Via homogeneous nucleation theory, we provide a criterion which determines growth of existing lead sulphate particles and the dissolution of new, smaller particles.

The outline of this paper is as follows. In Section 2 a model for the growth of a single, spherical lead sulphate particle is presented. The various temperature configurations are also highlighted. The governing concentration and particle radius equations are introduced in Section 3. The model for each of the temperature configurations is nondimensionalised in Section 4. The numerical results are discussed in Section 5.

2. Mathematical model

We consider a single, spherical lead sulphate particle with radius $r_p \equiv r_p(t)$ growing with time t in the acid solution. We apply a similar modelling approach used by Liger-Belair *et al.* [9] for the case of carbon dioxide bubble nucleation in champagne whereby we assume that the spherical domain around the particle nucleus can be approximated by two spherical subdomains: a relatively small boundary layer region around the particle (referred to as the diffusion region) and a larger far field well-mixed region (see Figure 1). The diffusion and well-mixed regions are characterised by time-independent and time-dependent lead concentration regimes, respectively. The radii of the diffusion and well-mixed regions are denoted r_d and r_w, respectively, such that $r_w \gg r_d$. We assume that the solution is sufficiently dilute such that particles interactions are negligible.

Assuming that the solution has an initial, constant lead concentration, C_0, the governing equations are

$$\frac{D}{r^2}\frac{\mathrm{d}}{\mathrm{d}r}\left(r^2\frac{\mathrm{d}C_d}{\mathrm{d}r}\right) = 0\,, \qquad \frac{\mathrm{d}C_w}{\mathrm{d}t} = 0\,, \tag{1}$$

where C_d and C_w are the lead concentrations in the diffusion and well-mixed regions, respectively, r is the radial coordinate, t is time and D is the diffusion coefficient for the lead atoms. At the interface of the diffusion region and the well-mixed region we prescribe

$$C_d(r_d) = C_w(r_d)\,, \qquad V_w\frac{\mathrm{d}C_w}{\mathrm{d}t} = -4\pi r_d^2 D\left.\frac{\mathrm{d}C_d}{\mathrm{d}r}\right|_{r=r_d}\,, \tag{2}$$

MURPHYS2016

IOP Conf. Series: Journal of Physics: Conf. Series **811** (2017) 012001

IOP Publishing

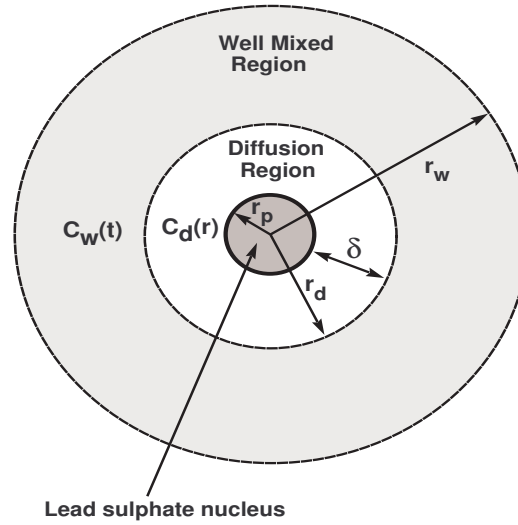doi:10.1088/1742-6596/811/1/012001

Figure 1. Lead sulphate particle with surrounding diffusion and well-mixed regions.

where V_w is volume of the well-mixed region. The first of these conditions represents lead concentration continuity condition, whilst the latter accounts for lead atoms diffusing between both regions. To track the surface of the particle we use the Stefan-type condition

$$\frac{\mathrm{d}r_p}{\mathrm{d}t} = DV_M \left.\frac{\partial C_d}{\partial r}\right|_{r=r_p} , \tag{3}$$

where V_M is the molar volume. The initial conditions are

$$r_p(0) = R_0 , \qquad C_w(0) = C_0 , \tag{4}$$

where R_0 is the initial particle radius.

The particle solubility is given by the Ostwald-Freundlich condition

$$C_d|_{r=r_p} = C^{EQ}(T) \exp\left(\frac{2\sigma V_M}{R_G T r_p}\right) , \tag{5}$$

where σ is surface tension, R_G is the universal gas constant and T is tank temperature.

From [10], the particle critical radius is

$$r_c = \frac{2\sigma V_M}{R_G T \ln\left(C_w/C^{EQ}\right)} , \tag{6}$$

where the particle grows if $r_p > r_c$ and dissolves if $r_p < r_c$. Hence, r_c acts as a criterion for whether particles will dissolve or grow, and hence can be used to ascertain the effectiveness of the particle settling process.

We consider three different temperature regimes, namely a constant temperature regime and two time-dependent temperature configurations. The process's current temperature configuration is defined by two temperatures: the initial temperature of the acid solution as it enters the tank, T_0 and the final steady state temperature of the solution, T_1. Whilst the initial temperature is fixed, the final temperature is adjustable. We note that for particle growth, we require $T_1 < T_0$. To model the present operating set-up, we assume that the acid solution

changes rapidly from T_0 to T_1. To investigate the effect of cooling the acid solution at slower rates than that of the current set-up, we define two monotonically decreasing time-dependent temperature functions

$$T_L = \begin{cases} T_0 + (T_1 - T_0)t/\tau & \text{if} \quad t \leq \tau \\ T_1 & \text{if} \quad t \geq \tau \,, \end{cases} \tag{7}$$

$$T_E = T_1 - (T_1 - T_0)\,\mathrm{erfc}\left(\frac{t}{\tau}\right), \tag{8}$$

where τ is a characteristic lead diffusion time scale associated with the constant temperature problem and erfc is the complementary error function. For the proceeding analysis the C, L and E subscripts denote terms pertaining to the constant, linear and error temperature models, respectively. Functions (7) and (8) are designed such that at time $t = 0$ (when the acid solution enters the tank) the temperature is equal to T_0. Thereafter the temperature decreases with time until the temperature is exactly equal to T_1 at $t = \tau$ for (7) and approximately equal to T_1 at $t = \tau$ for (8).

3. Solution
Solving the first equation of (1) leads to

$$C_d(r) = \frac{1}{r(r_p - r_d)}\left(r_d(r_p - r)C_w - C^{EQ}\exp\left(\frac{2\sigma V_M}{R_G T r_p}\right)r_p(r_d - r)\right), \tag{9}$$

where the concentration continuity condition in (2) and the solubility condition in (5) were used. Introducing (9) into the second interface condition in (2) yields

$$\frac{\mathrm{d}C_w}{\mathrm{d}t} = -\frac{3\,r_d\,r_p\,D}{r_w^3\,(r_p - r_d)}\left(C^{EQ}\exp\left(\frac{2\sigma V_M}{R_G T r_p}\right) - C_w\right), \tag{10}$$

where $V_W \equiv 4\pi r_w^3/3$ has been exploited. The particle radius equation is obtained by substituting (9) into the Stefan condition (3) to give

$$\frac{\mathrm{d}r_p}{\mathrm{d}t} = \frac{D V_M r_d}{r_p\,(r_p - r_d)}\left(C^{EQ}\exp\left(\frac{2\sigma V_M}{R_G T r_p}\right) - C_w\right). \tag{11}$$

4. Nondimensionalisation
4.1. Constant temperature model
Rewriting (10) and (11) in terms of the tank temperature T_1 and exploiting $\delta = r_d - r_p$ leads to

$$\frac{\mathrm{d}C_w}{\mathrm{d}t} = \frac{3\,D}{\delta r_w^3}\,r_p\,(r_p + \delta)\left(C^{EQ}(T_1)\exp\left(\frac{2\sigma V_M}{R_G T_1 r_p}\right) - C_w\right), \tag{12}$$

$$\frac{\mathrm{d}r_p}{\mathrm{d}t} = -\frac{D\,V_m}{\delta}\frac{r_p}{r_p + \delta}\left(C^{EQ}(T_1)\exp\left(\frac{2\sigma V_M}{R_G T_1 r_p}\right) - C_w\right). \tag{13}$$

We define the dimensionless variables

$$r_p = R_p\,\hat{r}_p\,, \qquad t = \tau\,\hat{t}\,, \qquad C_w = C_0\,\hat{C}_w\,, \tag{14}$$

where the unknown time scale τ is found presently. Substituting (14) into (12) yields

$$\frac{\mathrm{d}C_w}{\mathrm{d}t} = \tau\frac{3DR_p^2}{\delta r_w^3}\,r_p\,(r_p + \Delta)\left(H_C\exp\left(\frac{G_C}{r_p}\right) - C_w\right), \tag{15}$$

where the dimensionless notation has been dropped immediately, $\Delta = \delta/R_p = \mathcal{O}(1)$, $H_C \equiv \exp\left(B(T_1 - T_0)\right) = \mathcal{O}(1)$ and $G_C \equiv (2\sigma V_M)/(R_G R_p T_1)$. The last of these parameters is typically small for micron-sized particles. However, this is generally not the case for nanoparticles where R_p is small, and thus $G_C = \mathcal{O}(1)$. Hence, to keep the model general and applicable to particles of any size, we do not exploit the magnitude of G_C to make any reductions. We assume that the radius of the well-mixed region is related to the particle radius length scale via $r_w = \beta R_p$ where β is a measure of the distance between particles in the tank. The value of β depends on the diluteness of the solution where larger values of β yield larger well-mixed regions, and thus less lead sulphate nuclei in the tank. The time scale is found by balancing the parameters in (15) to give $\tau = (\beta^3 R_p \delta)/(3D)$. Thus,

$$\frac{\mathrm{d}C_w}{\mathrm{d}t} = r_p (r_p + \Delta) \left(H_C \exp\left(\frac{G_C}{r_p}\right) - C_w \right). \tag{16}$$

Introducing (14) into (13) leads to

$$\frac{\mathrm{d}r_p}{\mathrm{d}t} = -F_C \frac{r_p}{r_p + \Delta} \left(H_C \exp\left(\frac{G_C}{r_p}\right) - C_w \right), \tag{17}$$

where $F_C \equiv (\beta^3 V_M C_0)/3$. The initial conditions for each of the discussed temperature regimes are

$$C_w(0) = 1, \qquad r_p(0) = 1. \tag{18}$$

4.2. Time-dependent temperature models
Substituting the dimensionless time variable into the temperature functions (7) and (8) yields

$$T_L = \begin{cases} T_0 + (T_1 - T_0)t & \text{if } t \leq 1 \\ T_1 & \text{if } t \geq 1, \end{cases} \tag{19}$$

$$T_E = T_1 - (T_1 - T_0)\,\mathrm{erfc}\,(t), \tag{20}$$

where again the dimensionless notation has been negelcted. For $t \leq 1$ the dimensionless linear temperature problem is

$$\frac{\mathrm{d}C_w}{\mathrm{d}t} = r_p (r_p + \Delta) \left(H_L(t) \exp\left(\frac{G_L}{T_L(t)r_p}\right) - C_w \right), \tag{21}$$

$$\frac{\mathrm{d}r_p}{\mathrm{d}t} = -F_C \frac{r_p}{r_p + \Delta} \left(H_L(t) \exp\left(\frac{G_L}{T_L(t)r_p}\right) - C_w \right), \tag{22}$$

where $G_L \equiv (2\sigma V_M)/(R_G R_p)$ and $H_L(t) \equiv \exp\left(B(T_1 - T_0)t\right)$. The initial conditions remain unchanged from the constant temperature case. For $t \geq 1$ the dimensionless linear problem is just the constant temperature equations (16) and (17) with $C_w(1) = C_{t_1}$, $r_p(1) = R_{t_1}$ where C_{t_1} and R_{t_1} are the lead concentration and the particle radius, respectively, at $t = 1$.

Similarly, the dimensionless error function temperature problem is

$$\frac{\mathrm{d}C_w}{\mathrm{d}t} = r_p (r_p + \Delta) \left(H_E(t) \exp\left(\frac{G_E}{T_E(t)r_p}\right) - C_w \right), \tag{23}$$

$$\frac{\mathrm{d}r_p}{\mathrm{d}t} = -F_C \frac{r_p}{r_p + \Delta} \left(H_E(t) \exp\left(\frac{G_E}{T_E(t)r_p}\right) - C_w \right), \tag{24}$$

where $G_E \equiv G_L$ and $H_E(t) \equiv \exp\left(B(T_1 - T_0)\mathrm{erfc}(t)\right)$.

Table 1. Physical parameters used in simulations.

Meaning	Notation	Value	Units
Acceleration due to gravity	g	9.8	$\mathrm{m\,s^{-2}}$
Universal gas constant	R_G	8.31447	$\mathrm{J\,K^{-1}\,mol^{-1}}$
Lead sulphate density	ρ_{LS}	6290	$\mathrm{kg\,m^{-3}}$
Lead sulphate molar volume	V_M	4.821×10^{-5}	$\mathrm{m^3\,mol^{-1}}$
Lead diffusion coefficient	D	9.45×10^{-10}[13]	$\mathrm{m^2\,s^{-1}}$
Acid solution kinematic viscosity	ν_S	1.1×10^{-5}	$\mathrm{m^2\,s^{-1}}$
Acid solution dynamic viscosity	μ_S	0.021	$\mathrm{N\,s\,m^{-2}}$
Initial acid solution velocity	v_p	10	$\mathrm{m\,s^{-1}}$
Average lead sulphate particle radius	R_p	10^{-5}	m
Surface energy	σ	8.01×10^{-2} [14]	$\mathrm{J\,m^{-2}}$
Initial lead concentration	C_0	0.0128	$\mathrm{mol\,m^{-3}}$
Initial acid solution temperature	T_0	333	K
Final acid solution temperature	T_1	283	K
Equilibrium concentration fitting parameters	A, B	$2 \times 10^{-6}, 0.03$	$\mathrm{mol\,m^{-3}, K^{-1}}$
Width of diffusion region	δ	10^{-4}	m
Well mixed region parameter	β	75	-

5. Results

In this section the results of the model are discussed. The equations for the fixed and time-dependent temperature cases were simulated numerically in Matalab. Table 1 summarises the main physical and dimensionless parameters of the problem. The temperature-dependent equilibrium concentration $C^{EQ}(T) = A \exp(BT)$ is obtained by fitting the function with the experimental data of Crockford and Brawley [11, 12] for lead sulphate solubility over a range of temperatures and sulphuric acid concentrations in aqueous solutions. The width of the diffusion region around the particle is approximated via Prandtl's boundary layer (see Appendix A). The well mixed-region parameter $\beta = \rho_w/R_p$ is obtained by considering the distance between particles (i.e., solution diluteness) and the average particle radius. Based on experimental data from our industrial collaborator we found $\beta = 75$.

Figure 2 shows numerical solutions for the dimensionless concentration and particle radius subject to the fixed temperature (blue), linear temperature profile (green) and error function temperature configurations. We note that the difference between the three temperature configurations with respect to growth is negligible. The graphs demonstrate the correct qualitative behaviour where the lead sulphate particle grows via the flux of lead atoms, and hence the lead concentration in the well-mixed region decreases. Particle growth ends when a dynamic equilibrium between the particle and the lead atoms in the acid solution is attained. The simulations show that after 3 units of dimensionless time (or approximately 11.5 h) the concentration in the well-mixed region reaches a steady state and the particle has achieved its maximum size. Figure 2(b) also shows that there is a minimal increase of approximately 1.7% in particle radius during growth. This increase can be attributed to the small dimensionless parameter F_C in the particle radius equation. The F_C parameter depends on β where we note that larger values of β indicate the presence of less lead sulphate particles and consequently, less competition for lead atoms, which in turn leads to larger lead sulphate particles. However,

the cubic dependence of the time scale τ on β implies that larger nuclei require much longer to grow.
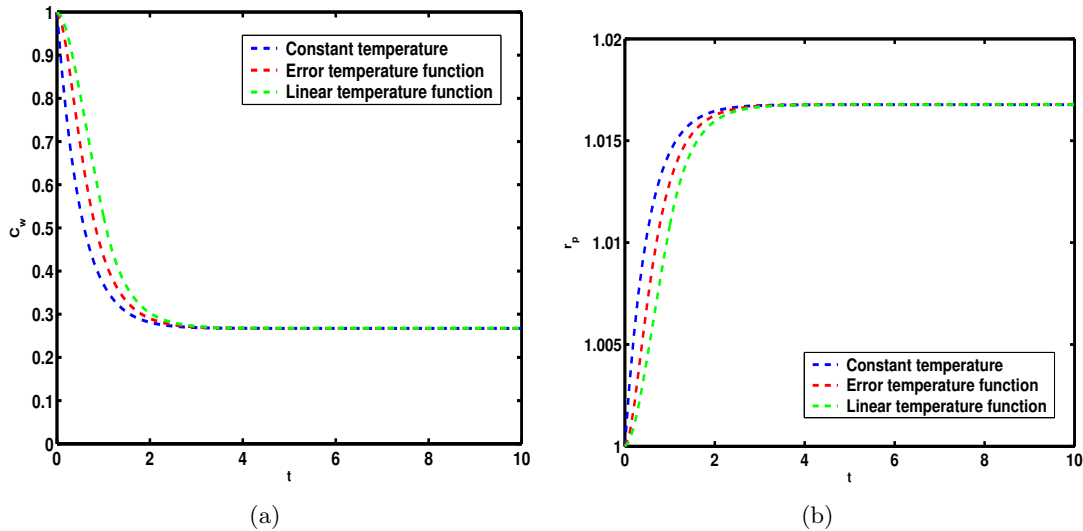

Figure 2. Evolution of (a) well-mixed region lead concentration and (b) lead sulphate particle radius subject to constant temperature (blue), error function temperature (red) and linear temperature function(green).

The critical radius evolution for each of the temperature configurations is shown in Figure 3. The curves divide regions which support particle growth (above curves) and particle dissolution (below curves). Initially the time-dependent temperature configurations have higher critical radii than that of the constant temperature regime. Thus, the former temperature set-ups are preferable as it is more difficult for new particles to precipitate out of solution due to the higher critical energy barrier. Unlike the other two curves, the constant temperature curve is monotonically increasing. For the constant temperature case when the acid solution enters the tanks its temperature decreases rapidly. This causes the lead sulphate solubility to decrease dramatically and thus the initial particle critical radius at $t = 0$ drops instantaneously to its minimum value. On the other hand, for the time-dependent temperature cases, the acid solution is subject to a slower cooling regime. Hence, the lead sulphate solubility limit decreases at a slower rate and reaches it minimum after approximately 0.7 units of dimensionless time (or 2.7 h). As the settling process proceeds to the point and beyond where the constant temperature curve intersects with the other two curves, we can see that the constant temperature configuration is an improvement on the other two temperature regimes.

6. Conclusion

In this paper we investigated the effect that temperature has on a lead sulphate settling process from the glassware manufacturing industry. A similar strategy to that proposed by Liger-Belair *et al.* [9] for modelling bubble nucleation from cellulose fibers in carbonated beverages was applied. The spherical region around the particle was divided into two separate regions each with its own characteristic lead atom diffusion regime. Specifically, the relatively small boundary layer region in contact with the particle was characterised by position-dependent diffusion and the larger (fast diffusion), far field well-mixed region was typified by time-dependent lead diffusion (slow diffusion). The final model consisted of two coupled nonlinear ordinary differential equations for the particle radius and the far-field concentration.
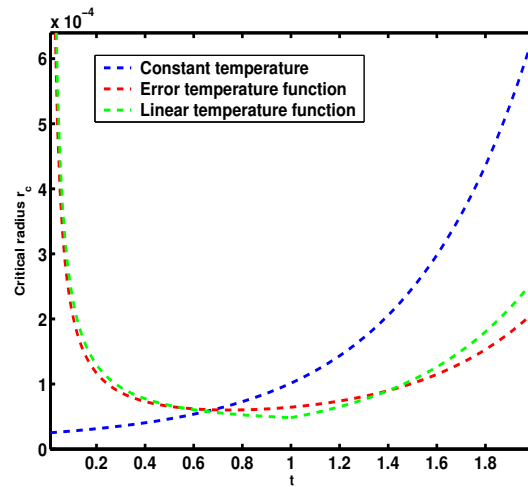
Figure 3. Evolution of dimensionless critical radius subject to constant temperature (blue), error function temperature (red) and linear temperature function (green).

Three temperature configurations were considered. The numerical simulations demonstrated minor particle growth. Furthermore, the time required for the particle to reach its maximum size was of the order hours. From an operating perspective, the acid solution should be allowed to sit overnight to maximise lead sulphate extraction. The small lead diffusion coefficient is one reason for the length in time required to achieve maximum particle growth. The introduction of a stirring mechanism, at least of the upper solution layers, could speed up the lead diffusion process.

An expression for the particle critical radius was also formulated. The time-dependent temperature configurations were shown to improve on the constant temperature case near the start of the process where particles had more difficulty overcoming the critical energy barrier associated with the former temperature regimes compared to the latter. However, as settling continues the performance of the constant temperature configuration was shown to be the best of the three configurations with respect to the dissolution of smaller particles and the growth of existing crystals.

Acknowledgments

Appendix A. Boundary layer width
Appendix A.1. Introduction
In this section we quantify the width of the diffusion region, δ around the lead sulphate particle. In Appendix A.2 we apply Prandtl's boundary theory to obtain an approximate expression for δ. Prandtl's approximation depends on the velocities of the acid solution and the particle, both of which are random in nature. Thus, in Appendix A.3 we formulate a set of stochastic differential equations for their velocities. In Appendix A.4 we derive a Fokker-Planck equation for the joint probability density function for the root mean square particle-solution relative velocity, which is then used to find δ.

Appendix A.2. Boundary layer approximation
We approximate the width of the particle diffusion region via Prandtl's boundary layer theory [15], which states $\delta \sim \sqrt{(\nu L)/U}$ where ν is the liquid kinematic viscosity, L is a characteristic length scale associated with the body which the liquid is flowing past and U is a liquid velocity scale. Thus, for the current study

$$\delta \sim \sqrt{\frac{\nu_S R_p}{u - v}}, \tag{A.1}$$

where ν_S is the acid solution dynamic viscosity and u, v are the velocities of the acid solution and particle, respectively. Assuming that the particle has a velocity component only in the vertical direction and negligible buoyancy, then via Newton's second law of motion, the one-dimensional equation for motion of a single spherical particle is

$$M_p \frac{\mathrm{d}v}{\mathrm{d}t} = -M_p g - F_D, \tag{A.2}$$

where g is gravity and M_p is particle mass. The drag force, F_D, depends on the acid solution flow regime, which in turn itself is charecterised by the magnitude of the Reynolds number $\mathrm{Re} = ((U - V)R_p)/\nu_S$. Using the parameter values in Table 1 and assuming that the difference between the acid solution and particle velocity scales U, V is $O(1)$ or less, then Re is presumed to be sufficiently small such that Stokes' law for the drag force is applicable. Thus, from [16]

$$F_D = -6\pi \mu_S R_p (v - u), \tag{A.3}$$

where μ_S is the solution kinematic viscosity. Upon substituting (A.3) into (A.2) we obtain

$$\frac{\mathrm{d}v}{\mathrm{d}t} = -g - \frac{1}{\tau_1}(v - u), \tag{A.4}$$

where $\tau_1 = M_p/(6\pi\mu_S R_p) \ll 1\,\mathrm{s}$ is a measure of the response time of the particle to interactions with the acid solution.

Appendix A.3. Acid solution velocity
The random motion of the acid velocity, and thus the interactions of the acid solution with the particle, is modelled via a time-dependent stochastic function. Specifically, we assume the solution velocity can be represented by a Gaussian stochastic function $u(t)$ with zero mean, variance $\langle u^2 \rangle = v_p^2$ and autocorrelation function

$$R(\delta t) = \langle u(t) u(t + \delta t) \rangle = v_p^2 \exp(-\delta t/\tau_2), \tag{A.5}$$

where we presume that the root mean squared acid solution velocity is equal to the initial velocity of the acid solution v_p (as imparted by the pump), $\delta t\,(> 0)$ is the time lag and τ_2 is the correlation time [17]. For the current system $\tau_2 = d/v_p$ where $v_p \approx 10\,\mathrm{m\,s^{-1}}$ is the acid solution velocity due to the pump and $d \equiv \sqrt{\nu_S t_{\mathrm{res}}} \approx 0.12\,\mathrm{m}$ is a length scale related to the size of the turbulent eddies in the solution. The time $t_{\mathrm{res}} \approx 1\,\mathrm{hr}$ corresponds to the residence time of the acid solution in the settlement tank and thus $\tau_2 \approx 0.03\,\mathrm{s}$.

To derive the stochastic differential equation (SDE) for u we begin by defining the realisation of the acid solution velocity at time $t + \delta t$ in terms of a deterministic and a completely random component. The deterministic part is dependent on the realisation of the acid solution at t and the time lag δt. Thus,

$$u(t + \delta t) = g(\delta t) u(t) + \sigma \xi(t), \tag{A.6}$$

where $g(\delta t)$ is an unknown function and σ is an unknown constant known as the average velocity per square-root time of the random fluctuations. The $\xi(t)$ term in (A.6) represents a completely random white noise process with zero mean. The autocorrelation function associated with $\xi(t)$ is $R(t) = \alpha^2 \delta(t)$ where α^2 is some positive constant and $\delta(t)$ is the standard Dirac delta function. We note that $\xi(t)$ is the time derivative of a Wiener process $W(t)$ such that

$$\xi(t) \;=\; \frac{dW}{dt}\,. \tag{A.7}$$

An expression for $g(\delta t)$ is obtained by multiplying $u(t)$ by $u(t + \delta t)$ and averaging over the ensemble of realisations to give

$$\langle\, u(t)\, u(t + \delta t)\,\rangle \;=\; \langle\, u(t)\,(g\, u(t) + \sigma \xi(t))\,\rangle \;=\; g\, v_p^2\,. \tag{A.8}$$

Comparing (A.5) with (A.8) it follows that $g(\delta t) = 1 - \delta t/\tau_2 + O(\delta t^2)$ for $t \ll 1$. Expanding (A.6) for small δt, diving through by δt and multiplying by dt yields

$$du \;=\; -\frac{u}{\tau_2}\, dt \;+\; \sigma'\, dW\,, \tag{A.9}$$

where $\sigma' = \sigma/\delta t$ and (A.7) has been exploited. To find σ' we first obtain $\langle u^2 \rangle$ via Itô's lemma [17], which states that for a SDE of the form

$$dx \;=\; a(x,t)\, dt \;+\; b(x,t)\, dW\,, \tag{A.10}$$

and any twice differentiable function $f(x,t)$ of two real variables x and t, then

$$df(x,t) \;=\; \left(\frac{\partial f}{\partial t} + a(x,t)\frac{\partial f}{\partial x} + \frac{1}{2}\, b(x,t)^2 \frac{\partial^2 f}{\partial x^2} \right) dt + b(x,t)\frac{\partial f}{\partial x}\, dW\,. \tag{A.11}$$

Hence, defining the new variable $f(u) = u^2$ and applying Itô's lemma to (A.9) yields

$$d(u^2) \;=\; \left(-\frac{2u^2}{\tau_2} + \sigma'^{\,2} \right) dt + 2\, u\, \sigma'\, dW\,. \tag{A.12}$$

An expression for σ' is found by considering a general mean-reverting stochastic process [18]

$$dS \;=\; a\,(L - S)\, dt \;+\; \sigma\, dW\,, \tag{A.13}$$

where a is the rate of mean-reverting. The solution to (A.13) tends to the equilibrium value, L with the stochastic term causing S to oscillate around L. Hence, (A.12) can be viewed as an equation for a mean-reverting stochastic process with $S = -(2u^2)/\tau_2$ and $L = \sigma'^{\,2}$, respectively. Thus, comparing terms in (A.12) yields $\sigma'^2 = (2\, u^2)/\tau_2$ or equivalently

$$\sigma' \;=\; v_p\, \sqrt{\frac{2}{\tau_2}}\,, \tag{A.14}$$

where we have exploited the fact that the magnitude of u^2 is $O(v_p^2)$. Introducing (A.14) into (A.9) yields the SDE

$$du \;=\; -\frac{u}{\tau_2}\, dt \;+\; v_p \sqrt{\frac{2}{\tau_2}}\, dW\,. \tag{A.15}$$

We define the dimensionless variables

$$v = v_p\, \hat{v} - \tau_1 g\,, \quad u = v_p \hat{u}\,, \quad t = \tau_2 \hat{t}\,, \quad W = \sqrt{\frac{\tau_2}{2}}\, \hat{W}\,, \tag{A.16}$$

which upon substitution into (A.4) and (A.15) yields

$$dv = \alpha\,(u - v)\, dt\,, \qquad du = -u\, dt + dW\,, \tag{A.17}$$

where the dimensionless notation has been dropped and $\lambda = \tau_2/\tau_1$.

Appendix A.4. Fokker-Planck equation and solution
We now formulate the Fokker-Planck associated with the joint probability density function of u and v. An arbitrary system of two SDEs in $x_1(t)$ and $x_2(t)$ is given by [19]

$$\frac{\mathrm{d}x_1}{\mathrm{d}t} = f_1(x_1, x_2) + g_1(x_1, x_2)\eta_1(t)\,, \qquad \frac{\mathrm{d}x_2}{\mathrm{d}t} = f_2(x_1, x_2) + g_2(x_1, x_2)\eta_2(t)\,, \qquad (A.18)$$

where $x_2(t)$ has autocorrelation $< x_2(t)x_2(t') >= \kappa \exp\left(|tt'|/\tau\right)$ and $\eta_1(t), \eta_2(t)$ are random force terms. The related two-dimensional Fokker-Planck equation for the joint probability density function of $x_1(t)$ and $x_2(t)$, P, is

$$\frac{\partial P}{\partial t} = -\frac{\partial}{\partial x_1}\left(f_1 P\right) - \frac{\partial}{\partial x_2}\left(f_2 P\right) + \kappa\frac{\partial}{\partial x_1}\left(g_1\frac{\partial}{\partial x_1}(g_1 P)\right) + \kappa\frac{\partial}{\partial x_2}\left(g_2\frac{\partial}{\partial x_2}(g_2 P)\right). \quad (A.19)$$

Hence, using $x_1 = v$, $x_2 = u$, $f_1 = \lambda(u - v)$, $f_2 = -u$, $g_1 = 0$ and $g_2 = 1$, the Fokker-Planck equation associated with (A.17) is

$$\frac{\partial}{\partial u}\left(uf\right) + \lambda\frac{\partial}{\partial v}\left((v - u)f\right) + \frac{\partial^2 f}{\partial u^2} = 0\,. \qquad (A.20)$$

where f is the stationary joint probability density function of u and v. If the first term in (A.20) is neglected, the resulting reduced equation has as its solution $g(u) = \exp\left(-u^2/2\right)$. Thus, we assume that the full solution to (A.20) can be written as $f(u, v) = g(u)h(u, v)$. The function $h(u, v)$ is determined via heuristic physical considerations regarding the nature of $f(u, v)$, and in particular the effect of the parameter λ on the relationship between u and v in (A.17). Firstly, inspection of the second SDE in (A.17) suggests that if $\lambda \gg 0$, then the particle velocity v tends towards the acid solution velocity u. Thus, in the limit as $\lambda \to \infty$ there is perfect correlation between u and v. On the other hand, as $\lambda \to 0$, the autocorrelation between u and v vanishes and v oscillates around its mean value. Assuming that the function h is exponential in nature, for intermediary values of λ we have $h(u, v) = \exp\left(-B[v - Au]^2\right)$ where A and B are unknown constants. Based on the above definition of $f(u, v)$, the function takes the form $f(u, v) = \exp\left(-u^2/2 - B[v - Au]^2\right)$. The constants A and B are found by substituting this expression for f into the Fokker-Planck equation and matching like coefficients for u and v to obtain

$$f(u, v) = \exp\left(-\frac{u^2}{2} - \frac{\lambda}{2}\left[u - \frac{\lambda + 1}{\lambda}v\right]^2\right). \qquad (A.21)$$

Finally, we average over the joint probability distribution of u and v to obtain the mean square particle relative velocity

$$\langle (u - v)^2 \rangle = \frac{\int_{-\infty}^{\infty}\int_{-\infty}^{\infty}(v - u)^2 f(u, v)\,\mathrm{d}u\,\mathrm{d}v}{\int_{-\infty}^{\infty}\int_{-\infty}^{\infty}f(u, v)\,\mathrm{d}u\,\mathrm{d}v} = \frac{1}{\lambda + 1}\,, \qquad (A.22)$$

which can be rewritten in dimensional terms via (A.16) and then used in (A.1).

References
[1] Montgomery JM 1985 *Water Treatment: Principles and Design* (John Wiley and Sons).
[2] Galvin KP 2010 Gravity separation of coal in the reflux classifier - new mechanisms for suppressing the effects of particle size *Int. J. Coal Prep. Util.* **30** 130-44.
[3] Laplante AR, Woodcock F and Noaparast M 1995 Predicting gravity separation gold recoveries *Miner. Metall. Proc.* **12** 74-9.

[4] Vettore L, De Matteis MC and Zampini P 1980 A new density gradient system for the separation of human red blood cells *Am. J. Hemat.* **8** 291-7.

[5] Ward J, Fowler AC and O'Brien SBG 2011 Acid polishing of lead glass *J. Math. Ind.*, **1** 1.

[6] Li Y, Kang JH, Lau SL, Kayhanian M and Stenstrom MK 2007 Optimization of settling tank design to remove particles and metals *J. Environ. Eng.-ASCE* **134** 885-94.

[7] Boon AG and Dolan JF 1995 Design of settlement tanks and the use of chemicals to aid precipitation of suspended solids *J. Chart. Inst. Water E* **9** 57-68.

[8] Agridiotis V, Forster CF and Carliell-Marquet C 2007 Addition of Al and Fe salts during treatment of paper mill effluents to improve activated sludge settlement characteristics *Bioresource Technol.* **98** 2926-34.

[9] Liger-Belair G, Voison C and Jeandet P 2005 Modeling nonclassical heterogeneous bubble nucleation from cellulose fibers: application to bubbling in carbonated beverages *J. Phys. Chem.* **109** 14574-80.

[10] Park J, Joo J, Kwon SG, Jang Y and Hyeon T 2007 Synthesis of monodisperse spherical nanocrystals *Angew. Chem-Ger. Edit.* **46** 4630-60.

[11] Crockford HD and Brawley DJ 1934 The solubility of lead sulfate in water and aqueous solutions of sulphuric acid *J. A. Chem. Soc.* **56** 2600-1.

[12] Crockford HD and Brawley DJ 1936 The solubility of lead Sulfate in aqueous solutions of sulfuric acid at high concentrations *J. Phys. Chem.-US* **40** 303-5.

[13] Lide DR 2006 *RC Handbook of Chemistry and Physics: A Ready Reference Book of Chemical and Physical Data* (Boca Raton, FL. , London).

[14] Bernardi DM 1990 Nucleation of lead sulfate in porous lead-dioxide electrodes *J. Electrochem. Soc.* **137** 1670-81.

[15] Ackroyd JAK, Axcell BP and Ruban AI 2001 *Early Developments in Modern Aerodynamics* (Butterworth-Heinemann Oxford).

[16] Fowler AC 1997 *Mathematical Models in the Applied Sciences* (Cambridge Texts in Applied Mathematics).

[17] Gardiner CW 2003 *Handbook of Stochastic Methods* (Springer Berlin).

[18] Van Kampen NG 2007 *Stochastic Processes in Physics and Chemistry* Elsevier.

[19] Risken H 1996 *The Fokker-Planck Equation: Methods of Solutions and Applications* (Springer, Berlin).